TUHH
Hamburg University of Technology

DRAFT Version

ICS
Institute of Control Systems

Master's thesis

# Beam orbit stability control in modern synchrotron light source facilities

*Author:*
Juan Gutiérrez Navarro

**Supervisor:** Dr. Ilya Agapov
M.Sc. Bindu Sharan
**Examiner:** 1. Prof. Dr. Herbert Werner
2. Dr. Annika Eichler

July 8, 2022

ICS
Institute of Control Systems

**Master's thesis** **M —3 — 2022**
for Mr. Juan Gutiérrez Navarro Student ID: 530752 Study Course: 2

**Title:**
**Beam orbit stability control in modern synchrotron light source facilities**

**Project Description:**
A Synchrotron light source is a type of x-ray source based on an electron storage ring.

At DESY in Hamburg, the PETRA IV project is upgrading the third-generation light source PETRA III to a fourth-generation light source with ultra-low emittance in order to reach the diffraction limit. Synchrotron light sources are used for scientific and technical purposes. The applicability of this technology extends across a wide range of scientific disciplines, such as physics, chemistry, biology, materials science, medicine, environmental science, and nanotechnology [1].

Synchrotron light storage rings are designed to achieve very small electron beam sizes. This allows synchrotron radiation to be as bright as possible. It is necessary to maintain tight tolerances in electron beam stability to make use of these small beam sizes. To achieve such stability, closed orbit control is important in the design and operation of light sources. Electron orbit fluctuations increase electron beam size and degrade photon beam brightness, while slower orbit deviations require frequent realignment of experiments at the end of photon beam lines [2].

Beam stability is one of the most important requirements in synchrotron light sources. Ambient vibrations and electrical noise cause orbit distortions which have to be counteracted by an orbit feedback [3]. In the case of PETRA IV, it will have a fast orbital feedback system (FOFB), with more than 700 beam position monitors and about 200 fast correctors [1].

The general objective of this work is to analyze the perturbations of the storage ring and simulate their effect on the feedback system. For this purpose, it will be first necessary to implement a model of the particle motion through the lattice with feedback system that keeps the trajectory within tolerable margins. Then, a model of the expected perturbations with the data obtained from seismic measurements at the ring will be include, And finally the performance of the feedback system will be evaluated.

**Tasks:**

1. Literature review
2. Create a software infrastructure in Python, with tools for the implementation of subsequent simulations of particle accelerators. For this purpose, new functionalities

will be implemented with the pyAT library. The necessary documentation will be prepared to make the infrastructure available to other users.

3. Identify the expected sources of disturbance. This will include experimental work on seismic measurements, data evaluation as well as analysis of pre-existing seismic data.
4. The data obtained in the previous step, will be input into the simulation model of the feedback system and the effect of perturbations analyzed.

# References


[1] C.G. Schroer et al. PETRA IV: upgrade of PETRA III to the Ultimate 3D X-ray microscope. Conceptual Design Report. Deutsches Elektronen-Synchrotron DESY, Hamburg, 2019.

[2] J. Safranek. Orbit control at synchrotron light sources. Conf. Proc. C, 991004:240–244, 1999.

[3] Gajendra Kumar Sahoo, Klaus Balewski, Winfried Decking, and Yongjun Li. Closed orbit correction and orbit stabilization scheme for the 6 gev synchrotron light source petra iii. EPAC-2004, Lucerne, pages 2302–2304, 2004.


**Supervisor:** Dr. Ilya Agapov
M.Sc. Bindu Sharan
**Examiner:** 1. Prof. Dr. Herbert Werner
2. Dr. Annika Eichler

**External:** DESY

**Deutscher Titel:** Stabilitätsregelung der Strahlenbahn einer Lichtquelle

**Start Date:** 01.04.2022
**Due Date:** 30.09.2022

02.05.2022, Prof. Dr. H. Werner

Hereby I declare that I produced the present work myself only with the help of the indicated aids and sources.

Hamburg, July 8, 2022 Juan Gutiérrez Navarro

# Abstract

To complete

# Contents

# 1 Introduction

To complete

# 2 Introduction to particle accelerators

This chapter will introduce the basic principles of the operation of a particle accelerator and its main components. In the second part, it will be introduced the particle beam steering from a linear beam optics approach.

## 2.1 How Particle Accelerators Work

## 2.2 Particle-Beam Dynamics

The interaction of charged particles with electromagnetic fields is called beam dynamics. In this section there will be an introduction to the linear approximation of these dynamics in which concepts needed in future sections will be defined.

### 2.2.1 Charged Particles in an Electromagnetic Field

The trajectory of charged particles is modified by electric and magnetic fields, through the Lorentz force

$$\boldsymbol{F} = q\boldsymbol{E} + q(\boldsymbol{v} \times \boldsymbol{B}). \tag{2.1}$$

In equation 2.1 the electric field is neglected because it is much more efficient to use magnetics fields to influence high-energy beams with a speed close to the speed of light.

To achieve a circular orbit it is necessary that the Lorentz force cancels the centrifugal force. Equating the two forces and assuming that the magnetic field is constant and transverse, the following expression is obtained:

$$qvB = \frac{mv^2}{\rho} \tag{2.2}$$

where $\rho$ is the radius of curvature of the trajectory, $q$ the charge of the particle and $m$ is the particle mass.

Dividing equation 2.2 by the velocity and regrouping the terms yields:

$$B\rho = \frac{p}{q} \tag{2.3}$$

where $p$ is the particle momentum and $B\rho$ is called beam rigidity [1].

In the following, transverse magnetic fields will be classified in a general way by separating them into series of multipoles. The objective is to understand the effect of a given magnetic field on the beam through the action of its different multipole components.

A Cartesian coordinate system (x, y, z) will be introduced to describe the motion of the particle. The direction of the beam is parallel to the z-axis and the transverse plane will be denoted as the (x, y) plane. It will be assumed that the motion of the particles are parallel to the z-axis and the magnetic field has only transverse components.

Because the transverse dimensions of the beam are small compared to the radius of curvature of the particle trajectory, the magnetic field can be expanded in the vicinity of the z-axis using Taylor series expansion

$$B_z(x) = B_{z0} + \frac{dB_z}{dx}x + \frac{1}{2!}\frac{d^2B_z}{dx^2}x^2 + \frac{1}{3!}\frac{d^3B_z}{dx^3}x^3 + ... \tag{2.4}$$

Substituting 2.4 in equation 2.3

$$\begin{aligned} B_z(x) = & \frac{q}{p}B_{z0} + \frac{q}{p}\frac{dB_z}{dx}x + \frac{q}{p}\frac{1}{2!}\frac{d^2B_z}{dx^2}x^2 + \frac{q}{p}\frac{1}{3!}\frac{d^3B_z}{dx^3}x^3 + ... \\ = & \underset{dipole}{\frac{1}{\rho}} + \underset{quadrupole}{kx} + \underset{sextupole}{\frac{1}{2!}k'x^2} + ... \end{aligned} \tag{2.5}$$

where k is the quadrupole strength.

In equation 2.5 it is observed that the magnetic field affecting the particle can be divided into different multipoles which have different effect on the particle path. The dipole have an effect on beam steering, the quadrupole on beam focusing and the sextupole on chromaticity compensation. If only the first two multipoles are considered we are in the field of linear optics since the bending forces are constant or increase linearly with the transverse displacement of the ideal trajectory [2].

### 2.2.2 Equation of Motion

To complete

### 2.2.3 Particle Trajectories and Transfer Matrices

To complete

### 2.2.4 Beta Function and Betatron Oscillation

To complete

### 2.2.5 Emittance

To complete

### 2.2.6 Tune

To complete

# 3 Problem Specifications

## 3.1 Orbit correction

Orbit stability is a crucial and import issue of modern generation light sources. Ambient mechanical and electrical noise cause rather large orbit distortions which have to be counteracted by an orbit feedback.

### 3.1.1 Instruments of Monitoring and Correction

In order to correct the orbit and locate the position of the particles it is necessary some instruments. In the case of PETRA, the FOFB system uses a star like structure in the cabling, where the position data, captured by the BPMs, is sent to a central processing unit. Calculations are performed in real time and digital output streams are sent to instrumentation buildings located around the ring. These streams are received by digital power amplifiers that ultimately feed the air coil correctors. The main instruments will be briefly discussed below [3].

#### Beam Position Monitors

The electron beam position by a sensors called Beam Position Monitors (BPM). Each monitor is composed by four electrostatic pick-up electrodes that are installed crosswise at the beam pipe wall. The electric field produced by the beam particles induces a charge on the electrodes. The difference signals of opposite electrodes yield the beam's centre of mass for both transverse planes, respectively. It is a non-destructive diagnosis (it does not affect the beam) [4] [5].

#### Corrector Magnets

Around the storage ring, dipole magnets called corrector magnets are used to correct the orbit. At a certain position and in a certain direction, each dipole contributes to the correction. The most effective correction is obtained when the correctors are located as near as possible to the sources of generating the largest orbit deviations, i.e. the quadrupoles [6].

### 3.1.2 Methods

To complete

## 3.2 System description

The objective of the FOFB is to mitigate fluctuations in the beam, which occurs mainly due to ground motion transmitted to the beam through the misalignment of the magnets.

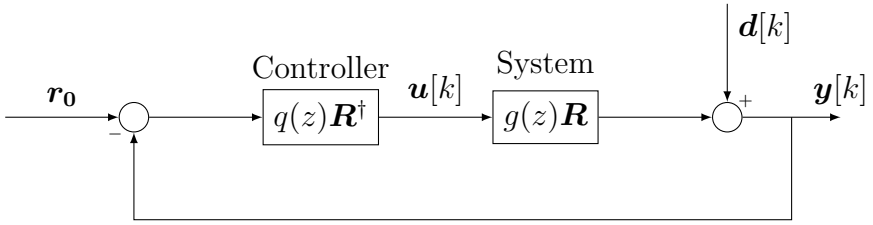


Figure 3.1: Schematic of the digital closed orbit feedback system.

To accomplish this task the control system modifies the correctors setpoints which is symbolized by $\boldsymbol{u}[k]$, where $k$ is the time index. The perturbations are introduced in the model by the vector $\boldsymbol{d}[k]$, the beam is steered back to the reference orbit $r_0$. The position of the beam is measured at each instant by means of BPMs located at different positions of the ring, the vector of the measurements is $\boldsymbol{y}[k]$.

The data obtained by the BPMs $\boldsymbol{y}[k]$ are used by the control algorithm to calculate the setpoint of the correctors $\boldsymbol{u}[k+1]$. The change in the monitors measurements $\boldsymbol{u}[k]$ due to changes in the actuators $\boldsymbol{u}[k]$ is modeled by a transfer function $g(z)$ that represent the dynamic response of the actuators and a static part which is a simple multiplication with the orbit response matrix $\boldsymbol{R}$. The schematic of the model is shown in 3.1 and can be written in the form

$$\boldsymbol{y}[k] = g(z)\boldsymbol{R}\boldsymbol{x}[k] + \boldsymbol{d}[k]. \tag{3.1}$$

In 3.1 we assume that $g(z)$ is the same for all the actuators since the same corrector magnets are used around the ring. The disturbances and the controller setpoints act on the BPM readings via different response matrix which will be discussed bellow.

## 3.3 Orbit Response Matrix

The orbit response matrix $\boldsymbol{R}$, is a linear relationship between a corrector magnet's strength (the extent to which it bends the beam) and the beam's position when measured horizontally or vertically by any "down-stream" Beam Position Monitor [7]. Therefore, the column i$^{th}$ of $\boldsymbol{R}$ correspond to the BPMs measurements if the corrector i$^{th}$ is excited with a unit step (1 $\mu rad$), is shown in 3.2. Theoretically, the linear response of a single dipole perturbation is the well-known closed orbit formula 3.2:

$$\Delta z(s') = \frac{\sqrt{\beta(s)\beta(s')}}{2\pi \sin(\pi\nu)} \Delta\theta \cos(|\phi(s) - \phi(s')| - \pi\nu) \tag{3.2}$$

where $z$ denotes the horizontal or vertical position, $\beta$, $\phi$ are the beta function and beta phase, $\nu$ is the tune [8]. It can be deducted that the orbit is proportional everywhere to the strength of the perturbation $\theta$ and to $\sqrt{\beta_o\beta_k}$ which is the amplitude of the beta function at the location of the perturbation.

If the process is repeated for all correctors and measured for all BPMs the spatial response matrix $\boldsymbol{R}$ is obtained. Although the matrix can be completely calculated theoretically

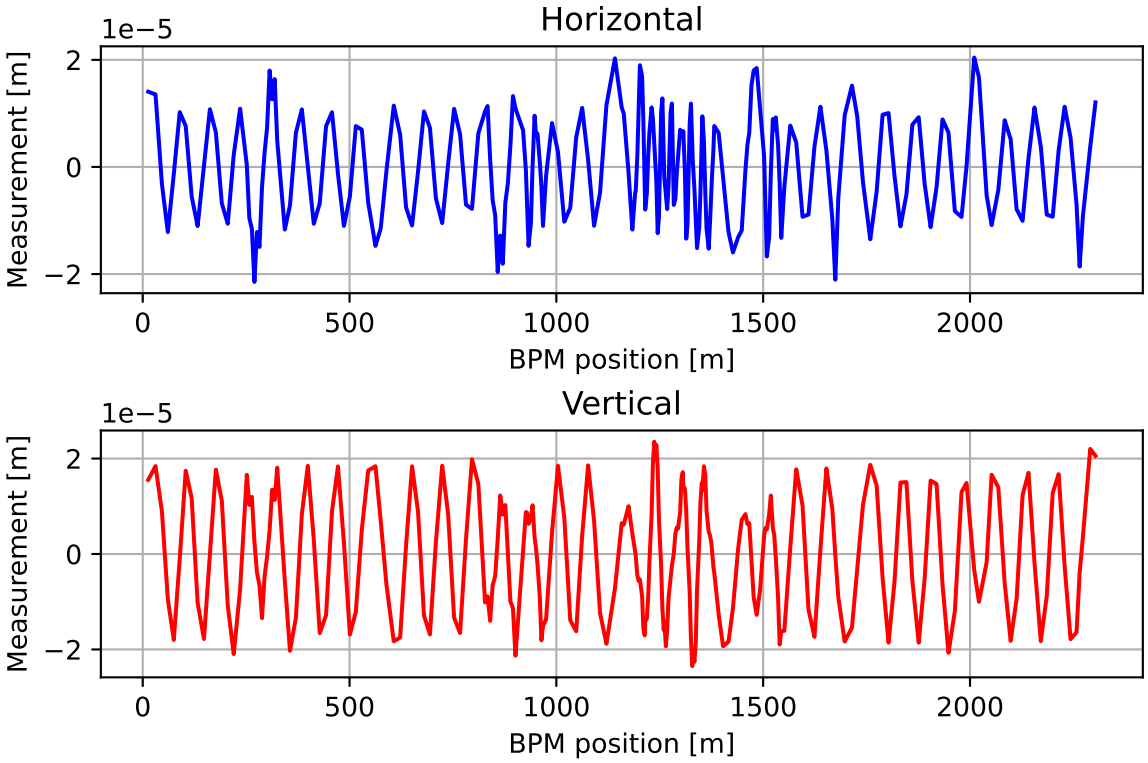


Figure 3.2: Readings of BPMs after applying a 1 $\mu m$ kick in the $1^{st}$ corrector.

using the accelerator model and physics, this methodology does not exactly represent the reality, for example, some misalignments of magnets or external magnetic perturbations would not be taken into account. It is a more common and accurate way to obtain it empirically directly on the actual ring [3].

In this thesis, to calculate the response matrix has been used a model of the PETRA III ring containing the information of each of its components and the tools of Accelerator Toolbox. By means of the function *find_orbit* [9] the particles are tracked through the ring simulation and the function of the closed orbit is obtained.

## 3.4 ORM inversion

## 3.5 Controller

### 3.5.1 Weighted SVD controller

The controller is divided between the time-dependent filter and the part that depends only on the direction of the measurement vector $\boldsymbol{y}[k] + \boldsymbol{d}[k]$ (spatial filter). The objective of the spatial filter is to reconstruct the system states $\boldsymbol{x}[k]$ (correctors setpoints) from the data obtained by the BPM measurements $\boldsymbol{y}[k]$ and to suppress the noise at the same time. Without the noise, $\boldsymbol{x}[k]$ can be perfectly obtained by multiplying $\boldsymbol{y}[k]$ by the pseudo-inverse

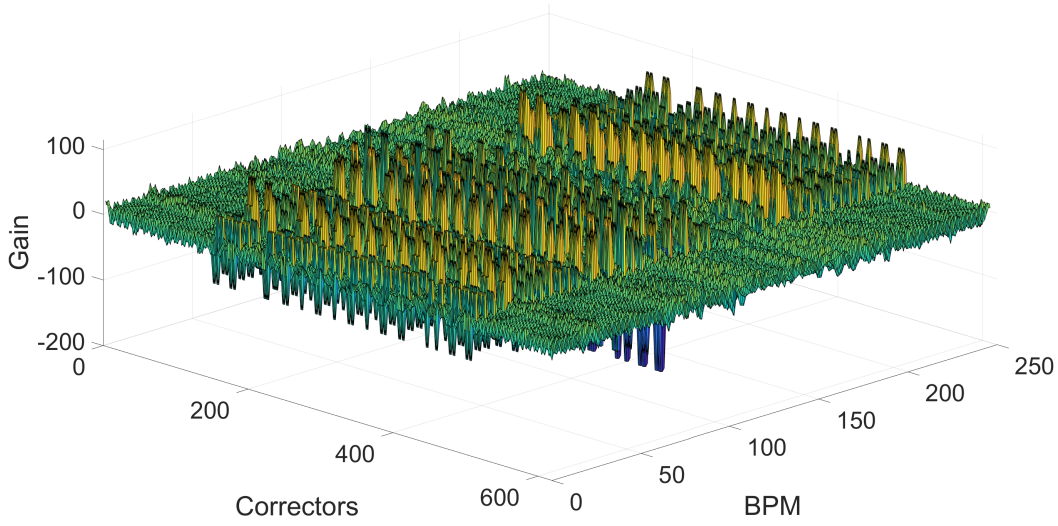


Figure 3.3: Storage ring response matrix 3D plot (horizontal).

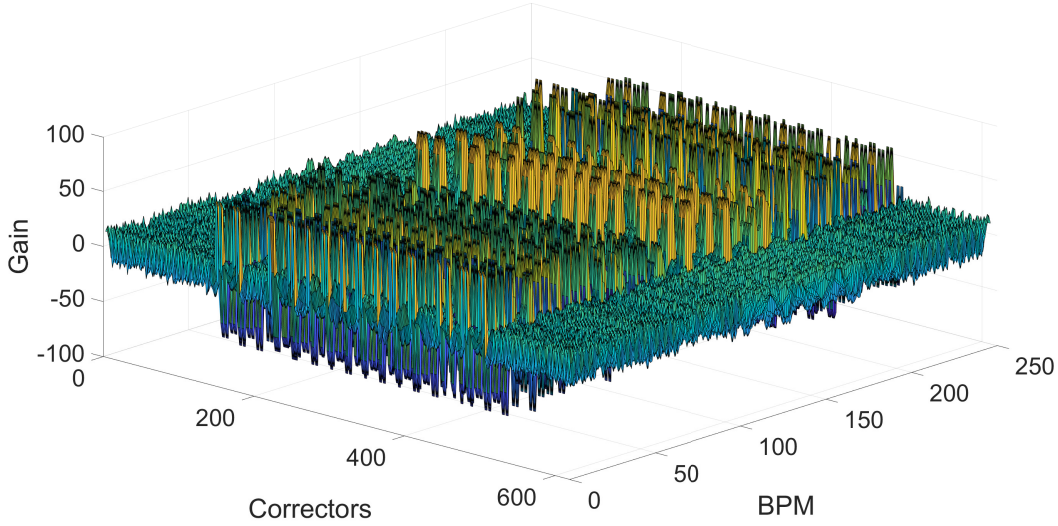


Figure 3.4: Storage ring response matrix 3D plot (vertical).

of the ring response vector $\boldsymbol{R}^{\dagger}$. However, the majority of synchrotron storage ring response matrices are ill-conditioned, this means that the condition number is very large. Practically, such a matrix is almost singular, and the computation of its inverse, or solution of a linear system of equations is prone to large numerical errors. A matrix that is not invertible has condition number equal to infinity [10].

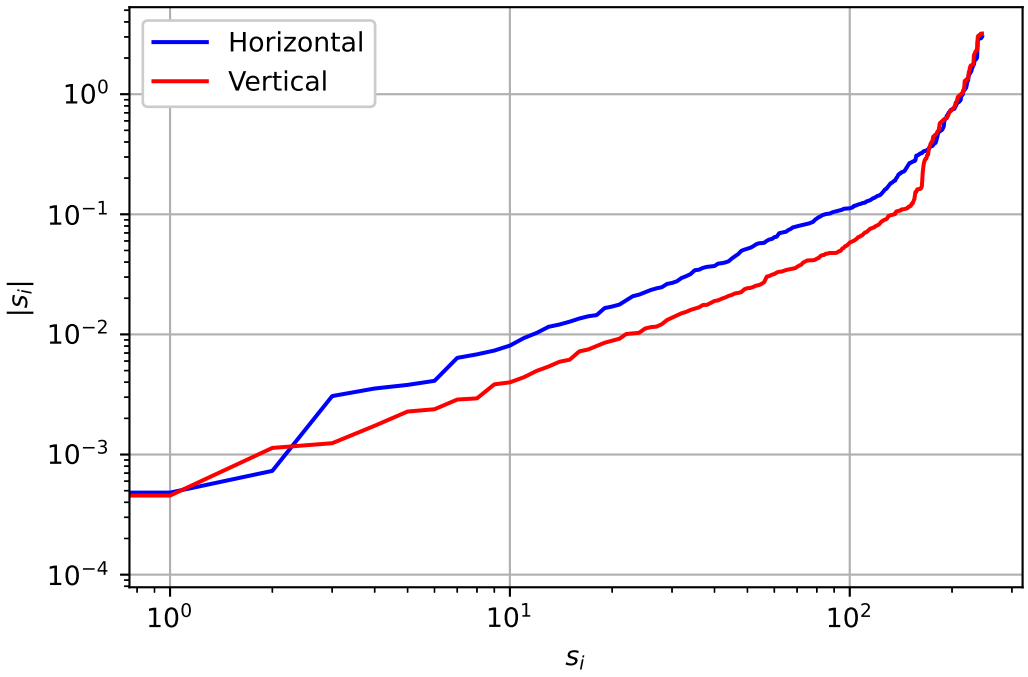


Figure 3.5: Magnitudes of the singular values $s[i]$ of the matrix $\boldsymbol{R}^\dagger$.

The condition number is the ratio of the largest to the smallest singular value:

$$\text{condition number} = \frac{s_1}{s_n} \tag{3.3}$$

[11]. To reduce the condition number of the pseudo-inverse of the response matrix $\boldsymbol{R}^\dagger$, the vector of measurements $\boldsymbol{y}[k]$ is multiplied by a modified matrix $\tilde{\boldsymbol{R}}^\dagger$ where the magnitudes of some of the singular values $s[i]$ have been reduced compared to $\boldsymbol{R}^\dagger$. To study which singular values $s[i]$ of $\boldsymbol{R}^\dagger$ have to be lowered, they are shown in figure 3.5. Most of the noise amplification occurs in the singular values with a high index $i$ and therefore a reduction of these values will result in less noise amplification.

Considering the facts that the first few $s[i]$ are able to mitigate the fluctuations in the beam and at the same time not amplify the noise too much, it is possible to create an efficient spatial filter. This is done by multiplying $\boldsymbol{y}[k]$ with $\tilde{\boldsymbol{R}}^\dagger = \boldsymbol{V}\boldsymbol{F}\boldsymbol{\Sigma}^{-1}\boldsymbol{U}^T$ where $\boldsymbol{F}$ is a diagonal matrix used to scale the singular values in $\boldsymbol{\Sigma}^{-1}$. In the case of the simulation of PETRA III the first 80 diagonal entries of of $\boldsymbol{F}$ are chosen to be 1, while all other entries are 0.

### 3.5.2 Correction

# 4 System and Correction Simulation

## 4.1 Modelling of Ground Effects

This section describes how a realistic ground motion model was created using the power density spectrum and the correlation between the motion of each quadrupole. This part is mainly based on [12].

Disturbances in the electron beam can cause degradation in luminosity due to beam displacement at the iteration point and emittance growth. The motion of the quadrupoles depends strongly on the correlation length of the ground motion. Therefore, the ground vibration model has to take into account not only the motion at a single point, but also the coherence properties of the ground motion. In addition, the model has to consider the circular shape of the machine.

The power spectrum $P_{tot}(w)$ of ground motion at a single point can be approximate by:

$$P_{tot}(w) = \frac{B}{w^4} \tag{4.1}$$

where $B$ is some proportionality constant characteristic of the site and $w = 2\pi f$. It it shown an example in 4.1. According to the ATL rule, the power spectrum $\rho(w, L)$ of the uncorrelated motion of two points at a distance L is:

$$\rho(w, L) = \frac{AL}{w^2}. \tag{4.2}$$

The uncorrelated part of motion must be smaller than the total motion, therefore

$$\rho(w, L) \leq P_{tot}(w) \text{ for all } w. \tag{4.3}$$

The coherent part of the motion of the $(n + 1)$st magnet with respect to the $n$th is obtained with first order lowpass filter with cutoff frequency $w_0 = \sqrt{B/(AL)}$ is

$$P_{corr,n+1}(w) = \left|\frac{w_0}{s + w_0}\right|^2 P_{tot,n}(w) = \left|\frac{w_0}{s + w_0}\right|^2 \frac{B}{w^4}. \tag{4.4}$$

And the uncorrelated motion obtained with a high pass filter with cutoff frequency of $w_0$ is

$$P_{uncorr,n+1}(w) = \left|\frac{s}{s + w_0}\right|^2 P_{n+1}(w). \tag{4.5}$$

To reflect the periodicity of the circular accelerator, it is necessary to correct the positions of all the magnets by

$$y_n{}^*(t) = y_n(t) - \frac{y_{N+1}(t) - y_1(t)}{L_{tot,N+1}} L_{tot,n} \tag{4.6}$$

where $L_{tot,n}$ is the total distance between 1st and the $n$th magnet

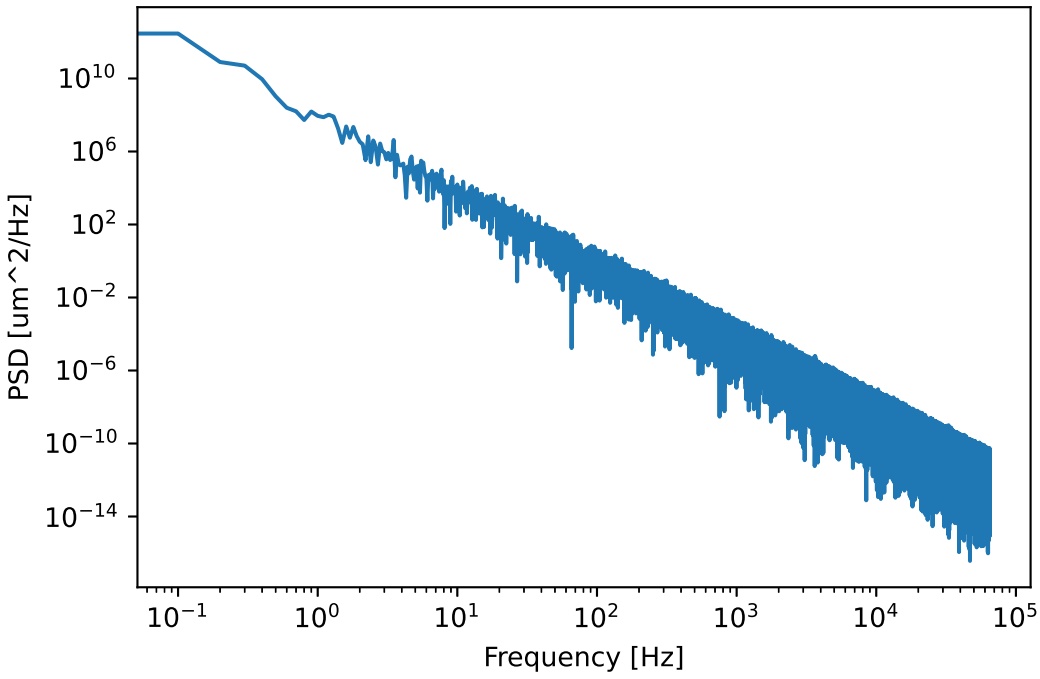


Figure 4.1: Simulated power spectrum at a single point.

## 4.2 Theorical Background

## 4.3 Simulation Model

## 4.4 Simulation Results

## 4.5 Robust Stability Analysis

## 4.6 pyAT

# 5 Conclusion and Outlook

To complete

# References


[1] B. Holzer, *Lattice design in high-energy particle accelerators*, en, 2014. DOI: 10.5170/CERN-2014-009.61. [Online]. Available: https://cds.cern.ch/record/1982419.

[2] K. Wille and J. McFall, *The Physics of Particle Accelerators: An Introduction*. Oxford University Press, 2000.

[3] J. Klute, H. Duhme, K. Balewski, H. Tiessen, and F. Wierzcholek, "The petra iii fast orbit feedback system", *DIPAC '11, Hamburg, Germany*, 2011.

[4] P. Forck, D. Liakin, and P. Kowina, "Beam position monitors", 2009.

[5] A. Gaupp and F. Wolf, "Beam position monitors", *Synchrotron Radiation News*, vol. 1, no. 3, pp. 27–31, 1988.

[6] *Fast horizontal and vertical correctors*, (Accessed on 07/04/2022). [Online]. Available: https://www.desy.de/~sahoo/WebPage/fast%20correctors.htm.

[7] G. White, T. Himel, and H. Shoaee, "A hybrid numerical method for orbit correction", in *Proceedings of the 1997 Particle Accelerator Conference (Cat. No. 97CH36167)*, IEEE, vol. 2, 1997, pp. 2425–2427.

[8] P. Chiu, C. Kuo, J. Chen, K. Hu, and K. Hsu, "Conceptual design and performance estimation of the tps fast orbit feedback system", Citeseer, 2008.

[9] ATcollab, *Welcome to pyat's documentation! — accelerator toolbox documentation*, https://atcollab.github.io/at/p/index.html, (Accessed on 07/03/2022).

[10] S. J. Leon, L. De Pillis, and L. G. De Pillis, *Linear algebra with applications*. Pearson Prentice Hall Upper Saddle River, NJ, 2006.

[11] J. Pillow, *Statistical Modeling and Analysis of Neural Data*. 2018, ch. Lecture 2 notes: SVD.

[12] C. Montag, "Simulation of ground motion induced proton beam orbit vibration in hera", in *Proceedings of the 1999 Particle Accelerator Conference (Cat. No. 99CH36366)*, IEEE, vol. 3, 1999, pp. 1566–1568.